INSTITUTE OF PHYSICS PUBLISHING JOURNAL OF PHYSICS B: ATOMIC, MOLECULAR AND OPTICAL PHYSICS

J. Phys. B: At. Mol. Opt. Phys. **38** (2005) 1987–1998 doi:10.1088/0953-4075/38/12/013

Single ionization and electron capture in He^{2+}+Na collisions

S Knoop[1], R E Olson[2], H Ott[1,3], V G Hasan[1], R Morgenstern[1] and R Hoekstra[1]

[1] KVI, Atomic Physics, Rijksuniversiteit Groningen, Zernikelaan 25, NL-9747 AA Groningen, The Netherlands
[2] Physics Department, University of Missouri–Rolla, Rolla, MO 65401, USA

E-mail: knoop@kvi.nl

Received 21 March 2005
Published 6 June 2005
Online at stacks.iop.org/JPhysB/38/1987

Abstract

Single-electron capture and ionization in He^{2+}+Na collisions at energies around the matching velocity (2–13 keV amu^{-1}) have been studied both experimentally and theoretically. State-selective cross section for capture into the $n = 2, 3, 4$ and $n \geqslant 5$, and the ionization cross section as well as differential cross sections for capture into $n = 3$ and 4 were obtained by the MOTRIMS method and compared with CTMC calculations. Good agreement was found between experiment and CTMC, especially concerning capture into high n-shells ($n = 4$, $n \geqslant 5$) and the ionization cross sections. For capture into the subdominant $n = 2$ shell close coupling calculations show better agreement. The differential cross sections for capture into $n = 3$ and 4 show a different energy dependency.

1. Introduction

Ever since the advent of highly charged ion sources, interactions between slow multicharged ions and atoms have been studied extensively. At low collision energies, electron capture dominates the interaction dynamics and therefore plays a significant role in man-made and astrophysical plasmas. In particular, photon emission following charge transfer reactions is an important diagnostics tool to determine properties of fusion plasmas [1, 2] and solar wind [3–6].

In general since one-electron capture proceeds mainly by transfer of the most loosely bound atomic electron, (quasi) one-electron models (see, e.g., [7]) are used to describe electron processes at low energies, i.e. velocities well below the classical orbiting velocity (v_{orb}) of the active electron.

[3] Present address: Institut für Physik, Johannes Gutenberg-Universität, Mainz, Germany.

 © 2005 IOP Publishing Ltd Printed in the UK

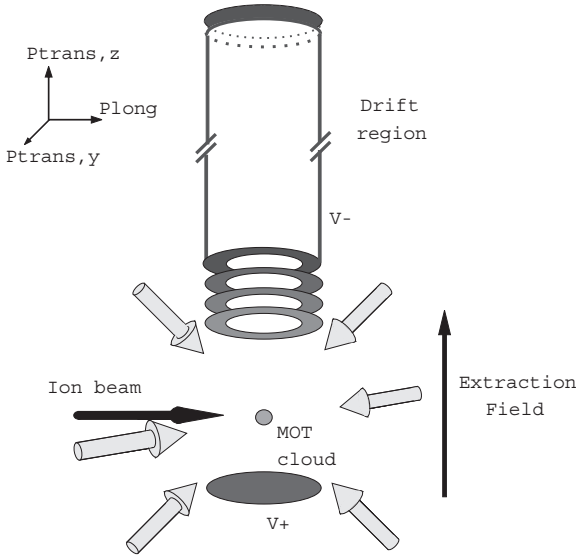

Figure 1. Schematic view of the experimental set-up. The magneto-optical trap consists of three sets of counterpropagating laser beam and two coils (not shown) producing the anti-Helmholtz magnetic field configuration. The Na^+ recoils are extracted upward in a weak electric field (<1 V cm^{-1}) towards the 2D detector.

Next to the real one-electron systems of fully stripped ions interacting with atomic hydrogen, collisions of fully stripped ions with alkali atoms are the most studied pseudo one-electron systems. One of the benchmark system is He^{2+}+Na(3s), which has been studied by a whole arsenal of experimental methods: charge-changing measurements, both non-coincident [8] and coincident [9], translational energy spectroscopy (TES) [10, 11] and photon emission spectroscopy (PES) [12–14]. A similar variety of theoretical methods has been used to investigate one-electron capture processes in He^{2+}+Na(3s) collisions, including close coupling [10, 15–17] and classical trajectory Monte Carlo (CTMC) methods [14].

Here, we present a systematic study of state-selective one-electron capture and ionization in He^{2+}+Na(3s) collisions at energies of 2–13 keV amu^{-1}. As the classical orbiting velocity of the Na(3s) electron corresponds to 9 keV amu^{-1} our energies cover the regime where the interactions change from being strongly dominated by state-selective capture to having many possible channels, including ionization. The technique of MOTRIMS (magneto-optical trapping recoil ion momentum spectroscopy) [18–21] is used, which is basically a COLTRIMS method [22] in which the cold target is provided by means of laser cooling and trapping. For support, the CTMC method has been used, which has been applied successfully to ion–alkali systems before [14, 23].

2. The MOTRIMS method

Since our MOTRIMS apparatus, which is depicted in figure 1, has been described elsewhere [24, 25] only a brief outline will be given here. Sodium atoms are cooled and trapped in a magneto-optical trap (MOT) forming a cloud of about 10^6 cold atoms in a volume of 1–5 mm^3. This cloud is crossed with an ion beam. The resulting Na^+ recoil ions are extracted in transverse direction by means of a weak electric field (<1 V cm^{-1}) towards the detector where both the

Table 1. Q-values and longitudinal momenta for the relevant n-shells in $He^{2+} + Na(3s) \rightarrow He^{+}(n) + Na^{+}$ for 4 keV amu^{-1} and 13 keV amu^{-1} projectile energy. Also the ionization potential is given, where the corresponding longitudinal momenta give the boundary between capture and ionization in the recoil spectra.

		p_{long} (au)	
n	Q-value (eV)	4 keV amu^{-1}	13 keV amu^{-1}
2	−8.46	−0.98	−0.79
3	−0.91	−0.28	−0.41
4	1.74	−0.04	−0.27
5	2.96	0.07	−0.21
∞	$I_{\mathrm{p}} = 5.14$	0.27	−0.10

2D position and the time-of-flight are recorded. From this data the recoil momentum vector can be reconstructed. During the measurements the magnetic field of the MOT (field gradient $\sim$30 G cm^{-1}) is switched off so as to not to disturb the recoil ion trajectories. The off-period can be chosen as long as on the order of 5–10 ms because the density of the MOT cloud decays only slowly. During the off-periods the atoms' motion is still damped by optical molasses cooling by the laser beams. Synchronized with the ion beam pulses, the laser beams are switched off for short periods of about 30 μs to ensure that the ions interact with ground state Na(3s) only.

Because a RIMS experiment images the primary process of the ion–atom collision, both electron capture

$$He^{2+} + Na \rightarrow He^{+}(nl) + Na^{+}, \tag{1}$$

and ionization

$$He^{2+} + Na \rightarrow He^{2+} + Na^{+} + e \tag{2}$$

can be observed directly in the Na^{+} recoil spectra. Since the target is unpolarized, the collision system possesses cylindrically symmetry around the beam axis. Therefore, only the momenta in longitudinal (p_{long}) and transverse (p_{trans}) directions to the ion beam are relevant. The longitudinal momentum is associated with the Q-value, the energy gain or loss of the reaction, while the transverse momentum is a measure for the impact parameter [22].

Our experimental momentum resolution is 0.1 au (corresponding to 5 m s^{-1}) in the longitudinal and one of the transverse directions. From the longitudinal component of the Na^{r+} recoil momentum after (multi-)electron capture the Q-value of the collision can be deduced via the following relation (in atomic units):

$$p_{\mathrm{long}} = \frac{Q}{v_{\mathrm{p}}} - \frac{1}{2} r v_{\mathrm{p}}, \tag{3}$$

with Q the difference between the total binding energies before and after the reaction, v_{p} the velocity of the primary ion and r the number of transferred electrons. The momentum resolution corresponds to a resolution of 1–2 eV for the Q-value, depending on the projectile velocity. In table 1, the Q-values of the relevant shells and the corresponding longitudinal momenta for collision energies of 4 and 13 keV amu^{-1} are given.

While the longitudinal momentum is linked to the Q-value of the process, the transverse momentum gives access to the scattering angle:

$$p_{\mathrm{trans}} = m_{\mathrm{p}} v_{\mathrm{p}} \theta, \tag{4}$$

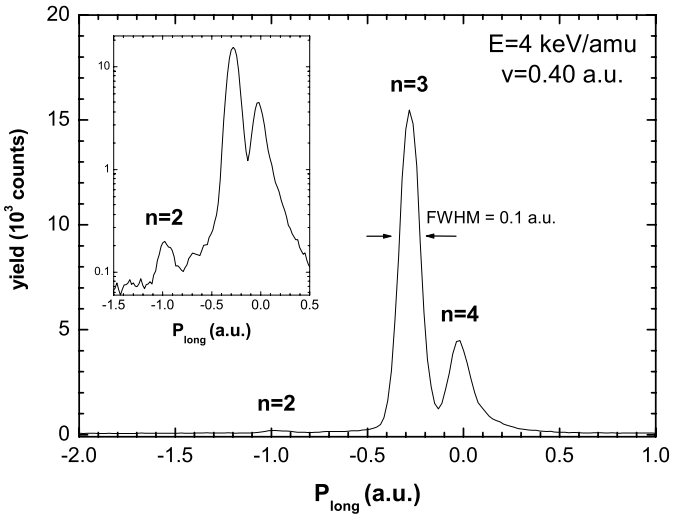

Figure 2. A longitudinal momentum spectrum of 4 keV amu^{-1} He^{2+}+Na(3s). Capture into $n = 3$ and $n = 4$ can be clearly separated. The inset shows the same spectrum on a log scale, for which capture into $n = 2$ can also be seen. The obtained resolution is 0.1 au.

where m_p and v_p are the mass and the velocity, respectively, of the projectile and θ the scattering angle. Equation (4) is valid for small angles, which for one-electron capture is always fulfilled ($\theta < 1$ mrad). From the transverse momentum distribution one can obtain the differential cross section (DCS). By selecting the transverse momenta within a specific longitudinal momentum bin the DCS for specific capture channels can be obtained.

Because of a better resolution in the position than in the time information (due to the finite ion pulse length) the transverse momentum distribution is deduced from the $p_{\mathrm{trans},y}$ position distribution alone. Due to the cylindrical symmetry around the beam axis the projection of the transverse momentum distribution onto the measured one ($p_{\mathrm{trans},y}$) is described by an Abel transformation [26]. Directly applying the inverse Abel transformation to obtain the transverse momentum distribution from $p_{\mathrm{trans},y}$ turns out to be quite sensitive to statistical noise. Therefore, we have applied a different, iterative method developed to extract velocity and angular distributions from two-dimensional ion/photoelectron imaging experiments [27].

A typical longitudinal momentum spectrum of Na^+ recoils is shown in figure 2. The resolution is mainly limited by imperfections in the electric field and not yet by the target temperature ($\sim$300 μK). The main capture channels ($n = 3$ and $n = 4$) can be separated and even the very weak $n = 2$ capture channel can be extracted. The longitudinal momenta are converted into Q-values via equation (3). Ionization of the Na atoms leads to values of Q larger than the ionization potential $I_P = 5.14$ eV. It can be shown that ionization events cannot appear at the capture side of the recoil spectrum, i.e., $p_{\mathrm{long}} \leqslant \frac{I_P}{v_p} - \frac{1}{2}v_p$. Therefore, $Q = I_P$ marks the Q-value boundary between capture and ionization contributions [28, 29]. Taking the experimental resolution into account and assuming a continuous decrease for $Q \to I$ ($n \to \infty$) the relative contributions of capture into high n-shells ($n \geqslant 5$) and ionization can be extracted.

From the Q-value spectra the relative cross sections of the different processes can be extracted. The partial cross sections for the relative contribution of capture into the $n = 2, n = 3$ and $n = 4$ shells are obtained by fitting Gaussian peaks to the spectra.

Subtracting these contributions from the total capture yield one obtains the partial cross section for capture into $n \geqslant 5$. Absolute calibration for all these channels is obtained by normalizing the total one-electron capture contribution to existing absolute cross sections [8–10], see section 4.

3. The CTMC method

The three-dimensional, three-body CTMC method employed here has been thoroughly described in the past [30, 31]. For application to a Na-atom target system, the Na(3s) electron is assumed to move in a model potential obtained from Hartree–Fock calculations [32]. Since the active electron is in the 3s-level, the microcanonical distribution was restricted to only allow angular momentum values between l and $l+1$, i.e. $l \leqslant 1$. For each collision energy, the coupled equations of motion are solved for 10^5–10^6 individual trajectories in order to obtain adequate statistics for the determination of the n-state-selective cross sections. For each of these trajectories, the initial electron orbits are randomized in such a way that the microcanonical distribution of momenta portrays the quantum mechanical distribution [30, 31, 33].

After each trajectory, collisions that result in electron capture are assigned to specific n-quantal levels using semiquantal binning procedures that have been developed and tested in previous work. For a hydrogenic projectile final state as in this case, the quantum defects are zero so that a classical number n_c is first determined from the binding energy of the electron, E_b, on the projectile in the post-collision regime

$$n_c = \frac{Z_A}{\sqrt{-2E_b}}. \tag{5}$$

Then, the non-integer n_c is related to the principal quantum number n of the final state by the condition [34]:

$$[n(n-0.5)(n-1)]^{1/3} < n_c \leqslant [n(n+0.5)(n+1)]^{1/3}. \tag{6}$$

The CTMC provides the complete momentum picture of the products after collision. For each trajectory that leads to a reaction under study, the momenta of the three bodies and their corresponding impact parameter are saved. These momenta are then used to predict the DCS in momentum space. The transverse momentum spectra for electron capture are, of course, directly related to the angular scattering of the projectile. In order to help illuminate the various collision dynamics, specific regions of momentum space can be binned to yield the impact parameters leading to the investigated phenomena.

4. Results and discussion

To put our MOTRIMS data on an absolute scale, a normalization procedure to absolute data is needed. Existing absolute, experimental data for one-electron capture from Na(3s) by He^{2+} ions [8–10] are shown in figure 3 together with results of the present CTMC calculations and of previous close coupling methods: 13-state atomic orbital expansion (AO13) [10], 45-state atomic orbital expansion (AO45) [15] and 74-state coupled-Sturmian-pseudostate expansion (SAO74) [17]. The total cross section shows an almost constant behaviour at low energies and a rapid decrease after 10 keV amu^{-1}. In general, there is good agreement between theories and experimental data, except that at energies above 10 keV amu^{-1} the SAO74 predict smaller cross sections.

From the comparison between the non-coincident and coincident data of DuBois and Toburen [8] and DuBois [9], respectively, it is clear that at least at lower energies there is no

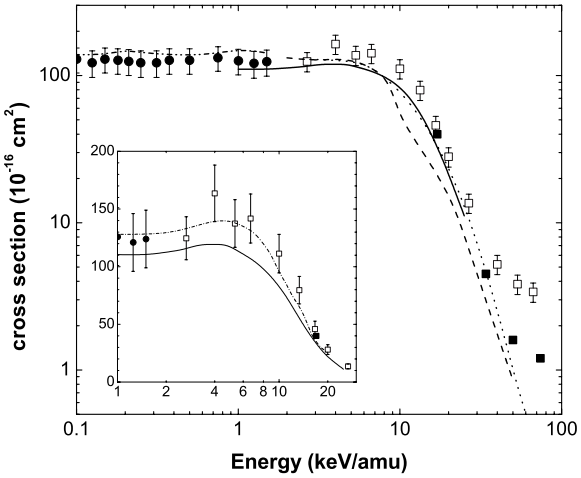

Figure 3. Absolute cross sections for one-electron capture in $He^{2+} + Na$. Experimental data: total He^+ production ((□) DuBois and Toburen [8] and (●) Schweinzer and Winter [10]), pure one-electron capture ((■) DuBois [9]). Theories on pure one-electron capture: (——) present CTMC, (— · · —) AO13 [10], (· · · · · ·) AO45 [15] and (- - - -) SAO74 [17]. The inset shows the 'recommended' curve (— · —) used to put our MOTRIMS data on an absolute scale (see the text).

significant contribution from transfer ionization to the single-electron capture cross sections. Therefore, in assessing the 'recommended' curve for total one-electron capture it was decided to follow the experimental data [8–10] and use a shape similar to the CTMC results. This implies that our normalization yields cross sections about 15% larger than the CTMC values.

4.1. State-selective cross section

A series of measured Q-value spectra is compiled in figure 4. With increasing projectile energy one clearly observes the increase of the capture into $n = 4$ and higher shells ($n \geqslant 5$) and of the ionization contribution to the spectrum. The relative, partial cross sections for capture into $n = 2, n = 3, n = 4$ and $n \geqslant 5$ and for ionization have been extracted from these Q-value spectra. As described above the relative cross section are made absolute by normalizing the sum of all capture channels to the recommended cross sections for one-electron capture (σ_{tot}), i.e.,

$$\sigma_n = \frac{\sigma_n^{\mathrm{rel}}}{\sum_n \sigma_n^{\mathrm{rel}}} \sigma_{\mathrm{tot}}. \tag{7}$$

In figure 5, the partial cross sections are shown and compared to the CTMC calculations, together with the AO45 and SAO74 close coupling methods.

Capture into the $n = 3$ state is the prime capture channel at low energy. Good agreement between MOTRIMS data and AO45, and SAO74 is observed. The CTMC data for $n = 3$ are about 20% too low. This difference is of similar order of magnitude as the difference between CTMC and the curve used for normalization of the MOTRIMS data (cf figure 3).

For capture into the $n = 4$ all theories and experiment exhibit a broad maximum around 7 keV amu^{-1}. The experimental maximum seems to be at a slightly higher energy than predicted by theory and, on average, the experimental data are somewhat lower at energies below the maximum and a bit higher at higher energies.

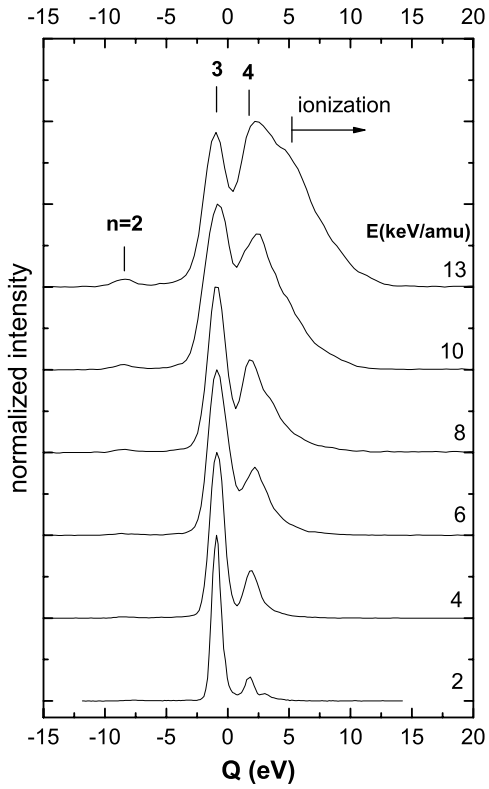

Figure 4. Overview of the Q-value spectra for different projectile energies. The Q-values of capture into $n = 2$, $n = 3$ and $n = 4$ as well as the onset of the ionization part are indicated. At low energy one-electron capture mainly takes place in the He^+ ($n = 3$) but with increasing energy capture into higher n-shells and ionization become important. As can be seen from equation (3) the resolution in the Q-value spectra decreases with projectile energy, from 0.9 eV at 2 keV amu^{-1} to 2.5 eV at 13 keV amu^{-1}, which can be seen in the broadening of the $n = 3$ capture peak.

Capture into higher n-shells could not be determined for individual n-shells but the sum of all channels with $n \geqslant 5$ could. The associated cross section peaks at approximately 10 keV amu^{-1}. Thus, as to be expected, it has a maximum at a somewhat higher energy than the $n = 4$ channel. The cross section for capture into the $n \geqslant 5$ is in good agreement with the CTMC results, while AO45 and SAO74 calculations underestimate this channel by almost one order of magnitude and do not reproduce the shape of it. It should be noted that these channels were not explicitly included in the AO45 and SAO74 approaches; their basis sets extended only up to the He^+(4f) level. The cross section for $n \geqslant 5$ was obtained by subtracting the contributions of the lower n channels from the total capture cross section. Inclusion of higher n-shells in the basis expansion could improve the theoretical results, but requires increasing calculation power. Clearly, this problem does not occur in CTMC approaches.

The small cross section for capture into the subdominant $n = 2$ state is in good agreement with the AO45 and SAO74 calculations, but is overestimated by a factor of 3 by CTMC. This electron channel has very little energy dependence.

In general we find good agreement between theory and experiment, although for high n-shells CTMC is in better agreement than AO45 and SAO74 while for the low levels the situation is reversed. The overestimation of the low n-values by the CTMC calculations

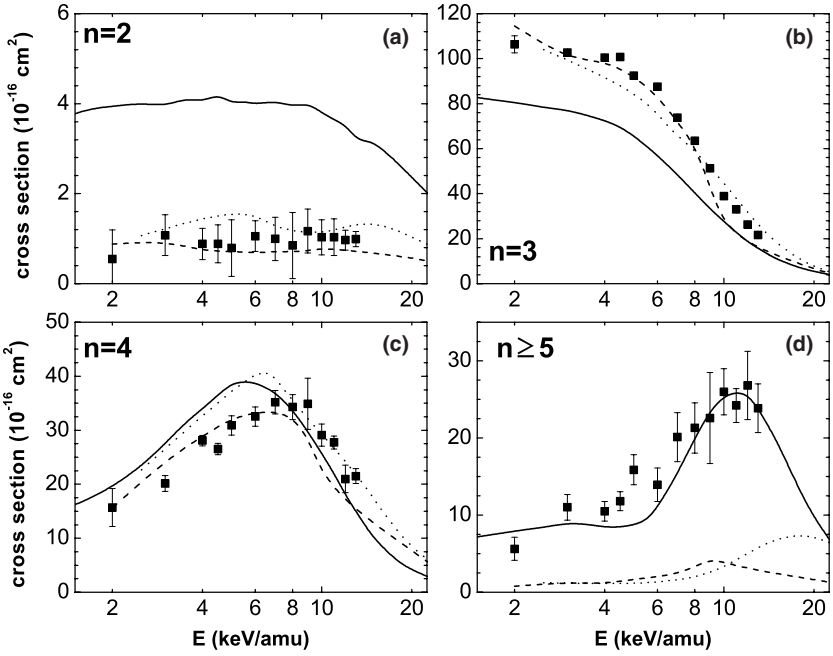

Figure 5. Partial cross sections for capture into $He^+(n)$ for (a) $n = 2$, (b) $n = 3$, (c) $n = 4$ and (d) $n \geqslant 5$. Theory: (——) CTMC, (· · · · · ·) AO45 [15] and (- - - -) SAO74 [17].

probably resides in the fact that multiple electron removal was not considered in this work. In a previous study [24] we found these channels are important and remove flux for single capture from the small impact parameters where the low n-value cross sections are born. Moreover, the CTMC method is expected to excel at predicting the high n-level capture and ionization cross sections since it is not restricted by basis set size and representation. Energetically, the energy loss for high n capture smoothly evolves to the ionization continuum, where in the next section we will see that the CTMC ionization cross sections are also in reasonable accord with experiment.

4.2. Ionization

The ionization cross sections are shown in figure 6. They have been determined by linkage to the electron capture cross sections in the following way:

$$\sigma_{\text{ion}} = \frac{\sigma_{\text{ion}}^{\text{rel}}}{\sum_n \sigma_n^{\text{rel}}} \sigma_{\text{tot}}. \tag{8}$$

The ionization is seen to increase very strongly, i.e., by a factor of ∼100 when the collision energy is increased from 2 to 13 keV amu^{-1}. The CTMC calculations are in reasonable agreement with the present MOTRIMS data, and nicely bridge the gap to the data by DuBois [9] at higher energy. The SAO74 calculations show agreement above 6 keV amu^{-1}, but do not reproduce the continuing decrease at lower energies.

Compared with the capture cross section which is almost constant at collision velocities below the classical orbital velocity of the active target electron (v_{orb}) and decreases at higher velocity, the ionization cross section increases rapidly around this orbital velocity and peaks between 20 and 30 keV amu^{-1}, which is ∼1.5v_{orb}. For energies below the ionization maximum

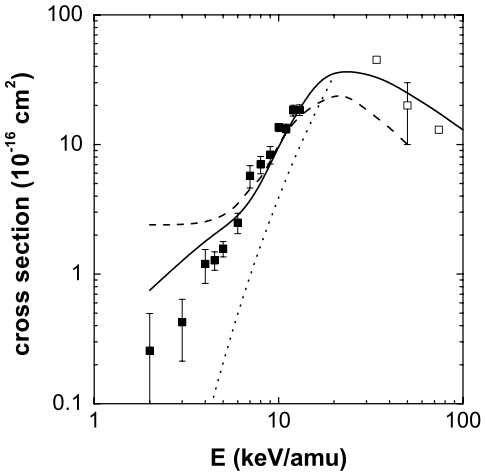

Figure 6. Cross sections for single ionization. (■) MOTRIMS, (——) CTMC, (□) DuBois [9], (– – –) SAO74 [17] and (· · · · · ·) scaling law for ionization [37].

scaling laws exist. They are based on ionization of H [36] and He [37] targets by highly charged ions. As discussed in [38], the scaling law proposed by Wu *et al* [37] is valid for both H and He targets at intermediate velocities ($v \leqslant 2.5v_{\rm orb}$). The result of applying the general form of the scaling law to the Na target is also shown in figure 6. It can be seen that the scaling law reproduces the shape of the cross section well, but is shifted to higher energies. This suggests that the scaling of the projectile velocity should be modified to include targets in which the electron is much less bound than in the case of H and He.

4.3. Differential cross section

Transverse momentum distributions or differential cross sections (DCS) are extracted from the recoil spectra for capture into the $n = 3$ and $n = 4$ shells. Although DCS in p+Na(3s, 3p) ([39] and reference therein) and in Li^++Na(3s, 3p) ([26] and reference therein) collisions have been studied intensively, for the present collision system only DCS in He^{2+}+Na($3p_{-1}$) have been studied theoretically with CTMC and atomic orbitals calculations by Dubois *et al* [40]. To our knowledge for the present collision system experimental DCS have not been reported.

In order to compare the experimental data and CTMC calculations the DCS are normalized to a peak value of one. In addition, the transverse momenta are scaled with the square root of the projectile energy. This removes the effect of the collision time on the spectral width, i.e., assuming pure Rutherford scattering. Therefore, in this representation, the abscissa is approximately inversely proportional to the impact parameter.

Figure 7 shows the transverse momentum distributions for different energies for capture into $n = 3$ and $n = 4$, both for the CTMC calculation as well as the MOTRIMS data. As a first remark one notes that at all energies, both for capture into $n = 3$ and $n = 4$, the calculations show a broader distribution towards larger transverse momenta as compared to the experimental distributions. Comparing the $n = 3$ and $n = 4$ channels, at low energies the CTMC results exhibit a broader distribution for the $n = 4$ shell, while at 10 keV amu^{-1} the $n = 3$ and $n = 4$ distributions are similar. With increasing projectile energy, the distribution of the $n = 3$ channel broadens towards larger scaled momenta while for the $n = 4$ channel the distributions remain almost unchanged. Both trends are also observed in the experiments.

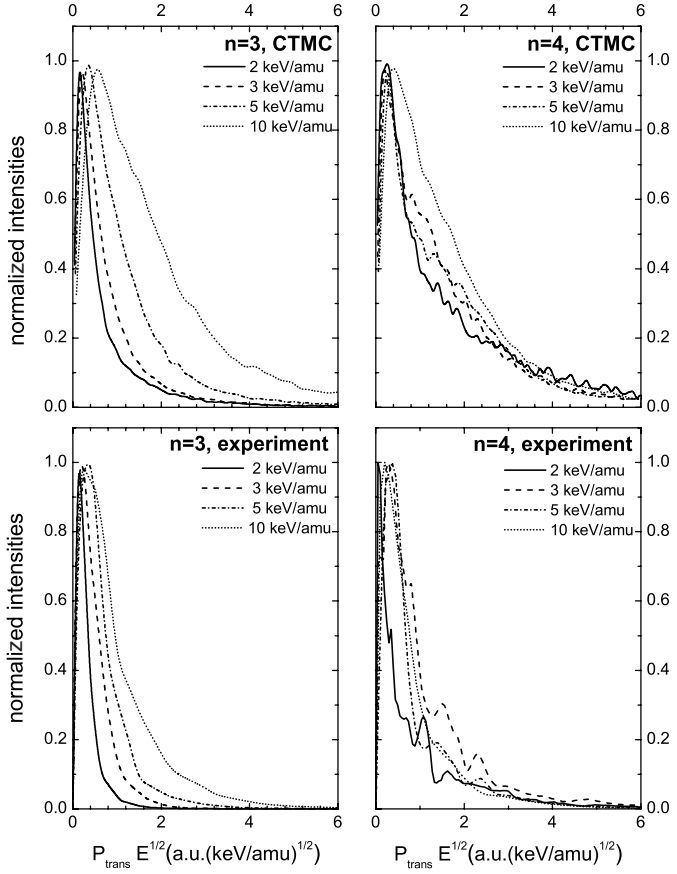

Figure 7. Transverse momentum distribution for capture into the $n = 3$ and $n = 4$ shells for 2, 3, 5 and 10 keV amu^{-1} projectile energy, present data and CTMC calculation. For comparison the maxima of both are normalized to one.

This implies that the effective impact parameters change to smaller distances for the $n = 3$ channel, but stay the same for the $n = 4$ channel. This seems to indicate that flux at larger impact parameters is drawn into the $n = 4$ channel at the expense of the $n = 3$ channel. As the $n = 4$ distribution does not change this implies that the coupling to the $n = 4$ channel becomes more efficient. From figure 5 it is seen that indeed the cross section for $n = 3$ decreases while the one for $n = 4$ increases for energies up to 10 keV amu^{-1}.

We also note that the maximum contribution to the n-selective cross sections peaks at very small scattering angle. Overall, the maxima are located at approximately 0.4 au (keV amu^{-1})$^{1/2}$. As an illustration, this value corresponds to a projectile scattering angle of 0.034 mrad at 10 keV amu^{-1}.

5. Conclusion

Single-electron capture and ionization in He^{2+}+Na collisions at energies around the matching velocity have been studied both experimentally and theoretically. Partial cross sections as well as differential cross sections were obtained by the MOTRIMS method and compared

with CTMC calculations. It was found that the cross sections for capture into high n-shells ($n = 4, n \geqslant 5$) are in best agreement with the CTMC results, while for capture into the subdominant $n = 2$ shell close coupling calculations show better agreement. The ionization cross sections show good agreement between experiment and CTMC, but deviate from a scaling law, which was proposed on the basis of ionization processes on H and He targets. The differential cross sections show a different energy dependency for capture into $n = 3$ and $n = 4$, which is confirmed by the CTMC calculation.

Acknowledgments

We gratefully acknowledge the support of the KVI technical staff. As project 99AQ03 this work is part of the research programme of the Stichting voor Fundamenteel Onderzoek der Materie (FOM) which is financially supported by the 'Stichting voor Nederlands Wetenschappelijk Onderzoek' (NWO). The participation of Dr Herwig Ott has been made financially possible by a visitors grant of the 'Stichting voor Nederlands Wetenschappelijk Onderzoek' (NWO). REO acknowledges the support of DOE—Office of Fusion Energy Sciences.

References

[1] von Hellermann M G *et al* 1993 *Plasma Phys. Control. Fusion* **35** 799
[2] O'Mullane M G, Mattioli M, Gianella R and Peacock N J 1999 *Plasma Phys. Control. Fusion* **41** 105
[3] Lisse C M *et al* 1996 *Science* **274** 205
[4] Beiersdorfer P, Olson R E, Brown G V, Chen H, Harris C L, Neill P A, Schweikhard L, Utter S B and Widmann K 2000 *Phys. Rev. Lett.* **85** 5090
[5] Beiersdorfer P *et al* 2003 *Science* **300** 1558
[6] Bodewits D, Juhász Z, Hoekstra R and Tielens A G G M 2004 *Astrophys. J.* **606** L81
[7] Fritsch W and Lin C D 1991 *Phys. Rev.* **202** 1
[8] DuBois R D and Toburen L H 1985 *Phys. Rev.* A **31** 3603
[9] DuBois R D 1986 *Phys. Rev.* A **34** 2738
[10] Schweinzer J and Winter H 1990 *J. Phys. B: At. Mol. Opt. Phys.* **23** 3881
[11] Gieler M, Aumayr F, Schweinzer J, Koppensteiner W, Husinsky W, Winter H P, Lozhkin K and Hansen J P 1993 *J. Phys. B: At. Mol. Opt. Phys.* **26** 2137
[12] Dehong Y, Jiarui L, Ziming L, Feng Y, Guangyan P, Duanwei W and Shiang S 1989 *Phys. Rev.* A **39** 2931
[13] Schlatmann A R, Hoekstra R, Folkerts H O and Morgenstern R 1992 *J. Phys. B: At. Mol. Opt. Phys.* **25** 3155
[14] Schippers S, Boduch P, van Buchem J, Bliek F W, Hoekstra R, Morgenstern R and Olson R E 1995 *J. Phys. B: At. Mol. Opt. Phys.* **28** 3271
[15] Shingal R, Noble C J and Bransden B H 1987 *J. Phys. B: At. Mol. Phys.* **19** 793
[16] Kumar A, Lane N F and Kimura M 1990 *Phys. Rev.* A **42** 3861
[17] Jain A and Winter T G 1996 *J. Phys. B: At. Mol. Opt. Phys.* **29** 4675
[18] Flèchard X, Nguygen H, Ben-Itzhak I, Wells E and DePaola B D 2001 *Phys. Rev. Lett.* **87** 123203
[19] van der Poel M, Nielsen C V, Gearba M-A and Andersen N 2001 *Phys. Rev. Lett.* **87** 123201
[20] Turkstra J W, Hoekstra R, Knoop S, Meyer D, Morgenstern R and Olson R E 2001 *Phys. Rev. Lett.* **87** 123202
[21] Nguyen H, Fléchard X, Brédy R, Camp H A and DePaola B D 2004 *Rev. Sci. Instrum.* **75** 2638
[22] Ullrich J, Moshammer R, Dorn A, Dörner R, Schmidt L P H and Schmidt-Böcking H 2003 *Rep. Prog. Phys.* **66** 1463
[23] Olson R E, Pascale J and Hoekstra R 1992 *J. Phys. B: At. Mol. Opt. Phys.* **25** 4241
[24] Knoop S, Turkstra J W, Morgenstern R, Olson R E and Hoekstra R 2003 *Nucl. Instrum. Methods* B **205** 560
[25] Knoop S, Morgenstern R and Hoekstra R 2004 *Phys. Rev.* A **70** 050702(R)
[26] van der Poel M, Nielsen C V, Rybaltover M, Nielsen S E, Machholm M and Andersen N 2002 *J. Phys. B: At. Mol. Opt. Phys.* **35** 4491
[27] Vrakking M J J 2001 *Rev. Sci. Instrum.* **72** 4048
[28] Dörner R, Mergel V, Jagutzki O, Spielberger L, Ullrich J, Moshammer R and Schmidt-Böcking H 2000 *Phys. Rep.* **330** 96
[29] Weber Th *et al* 2001 *Phys. Rev. Lett.* **86** 224

[30] Abrines R and Percival I C 1966 *Proc. Phys. Soc.* **88** 861
[31] Olson R E and Salop A 1977 *Phys. Rev.* A **16** 531
[32] Garvey R H, Jackman C H and Green A C S 1975 *Phys. Rev.* A **12** 1144
[33] Reinhold C O and Falcòn C A 1986 *Phys. Rev.* A **33** 3859
[34] Becker R C and MacKellar A D 1984 *J. Phys. B: At. Mol. Phys.* **17** 3923
[35] Olson R E 1981 *Phys. Rev.* A **24** 1726
[36] Janev R K, Ivanovski G and Solov'ev E A 1994 *Phys. Rev.* A **49** R645
[37] Wu W, Cocke C L, Giese J P, Melchert F, Raphaelian M L A and Stöckli M 1995 *Phys. Rev. Lett.* **75** 1054
[38] Wu W, Deveney E F, Datz S, Desai D D, Krause H F, Sanders J M, Vane C R, Cocke C L and Giese J P 1996 *Phys. Rev.* A **53** 2367
[39] Roller-Lutz Z, Wang Y, Lutz H O, Nielsen S E and DuBois A 2000 *Phys. Rev.* A **61** 022710
[40] Dubois A, Nielsen S E, Hansen J P and Wang J 2000 *J. Phys. B: At. Mol. Opt. Phys.* **33** L197